SVAT CALIBRATION OF POINT AND REGIONAL SCALE WATER AND ENERGY DYNAMICS

By

BRENT WHITFIELD

A THESIS PRESENTED TO THE GRADUATE SCHOOL
OF THE UNIVERSITY OF FLORIDA IN PARTIAL FULFILLMENT
OF THE REQUIREMENTS FOR THE DEGREE OF
MASTER OF ENGINEERING

UNIVERSITY OF FLORIDA

2003

ACKNOWLEDGMENTS

I would sincerely like to thank Dr. Jennifer Jacobs, chairperson of my supervisory committee, for all of her guidance and support throughout the project. I would also like to thank my committee members, Dr. Jasmeet Judge and Dr. Kirk Hatfield, for all of their valuable suggestions and encouragement. I am very appreciative for the help of Dr. Paul Houser and Dr. Matthew Rodell from NASA's Goddard Space Flight Center in Greenbelt, Maryland. I am grateful to Gerard Ripo, Sudheer Reddy Satti, Shirish Bhat, Aniruddha Guha, Enching Hsu, Siqing Liu and Jeremy Andrews for all of their help in data collection, analysis and peer review.

I am indebted to my girlfriend, Erica Zingone, for all of her encouragement and for providing me with a justification for taking monthly vacations to Atlanta, Georgia. I am grateful for my parents, Randy and Martha Whitfield, for the emotional and financial support afforded me throughout my education at the University of Florida. I would also like to thank my dog Jake Whitfield for his consistent allegiance and watchful eye over all of my work.

Research assistantship was provided by NASA NIP Grant NAG5-10567.

TABLE OF CONTENTS

Page

ACKNOWLEDGMENTS iii

LIST OF TABLES v

LIST OF FIGURES vi

ABSTRACT vii

CHAPTER

1. INTRODUCTION 1

2. MODEL COMPARISONS 6

3. STUDY AREA 11

4. SIMULATION DESIGN 15

Parameterization 15
Initialization 16
Forcings 17

5. RESULTS AND DISCUSSION 18

Soil Moisture 18
Soil Temperature 22
Surface Heat Fluxes 25

6. CONCLUSION 34

LIST OF REFERENCES 36

BIOGRAPHICAL SKETCH 42

LIST OF TABLES

Table page

1. Methodology for parameterization for CLM and LSP. 7

2. Characterization of land surface processes for CLM and LSP. 8

3. Instrumentation used in this study 14

4. Required atmospheric forcings for CLM and LSP 17

LIST OF FIGURES

Figure page

1. Log scale plot of variation of parameterized saturated hydraulic conductivity with depth below the surface for CLM and LSP 9

2. Water table depth with time from April 10th the June 20th. Experiment period from May 4th to May 17th. 12

3. Comparison of measured soil water characteristic curve with three soil water characteristic curves defined by modeled soil matric potential (SMP) and seven hydraulic conductivity (K) curves based on the Clapp and Hornberger relationship within the CLM parameterization scheme. 16

4. Comparison of measured soil moisture with CLM and LSP modeled soil moisture at a) 7.6 cm, b) 12.7 cm and c) 17.8 cm. 20

5. Comparison of measured subsurface soil temperature and CLM and LSP modeled soil temperature at a) 2.5 cm, b) 7.6 cm, c) 12.7 cm and d) 17.8 cm. 24

6. Comparison of modeled and measured surface fluxes for a) CLM net radiation and b) CLM and LSP latent heat flux. 30

7. Comparison of modeled and measured surface fluxes for a) CLM and LSP sensible heat flux and b) CLM and LSP ground heat flux. 31

8. Comparison of measured and modeled surface energy fluxes for a typical cloudy day, May 7th for a) Latent heat flux, b) Sensible heat flux and c) Ground heat fluxes. ...32

9. Comparison of measured and modeled surface energy fluxes for a typical clear day, May 13th for a) Latent heat flux, b) Sensible heat flux and c) Ground heat fluxes. .33

Abstract of Thesis Presented to the Graduate School
of the University of Florida in Partial Fulfillment of the
Requirements for the Degree of Master of Engineering

SVAT CALIBRATION OF POINT AND REGIONAL SCALE
WATER AND ENERGY DYNAMICS

By

Brent Whitfield

May 2003

Chair: Jennifer Jacobs
Major Department: Civil and Coastal Engineering

The Community Land Model (CLM) and the Land Surface Process model (LSP) are typical soil vegetation atmosphere transfer models (SVAT) that were used to simulate the land surface processes for a wet prairie community in the southeastern US for May 4-17, 2001. The research objective is to provide a basis for calibration of SVAT modeling processes for the highly variable convective atmospheric conditions and the atypical hydrogeology of the southeastern US. Since CLM is a watershed or regional scale model and LSP is a field scale model, each model has distinctive parameterization schemes and methodologies for simulating land surface processes. The intercomparison of CLM and LSP provides perspective for the strengths and weaknesses of the generalized parameterization schemes of a regional scale model as compared to a more biophysically adept field scale model. The study area is Paynes Prairie State Preseve in north-central Florida, which can be characterized by the biological communities of freshwater marsh, wet prairie and pasture.

Validation data were provided using standard meteorological instrumentation, an eddy correlation system for measurement of surface heat fluxes and subsurface measurements of moisture, temperature and matric potential. The CLM and LSP simulations of soil moisture at 7.6, 12.7 and 17.8 cm compared well with the measured results showing a RMSE less than 3.5% volumetric water content for both models at all three depths. Soil temperature simulations corresponding to 2.5, 7.6, 12.7 and 17.8 cm show good agreement with measured temperatures with a RMSE less than 1.5 K for all four depths in both simulations. Simulation of the components of the energy balance showed different trends for CLM than LSP. CLM's simulation showed the strongest agreement with the measured latent heat fluxes (RMSE of 62 Wm^{-2}) as compared with the simulation of sensible (RMSE of 61 Wm^{-2}) and ground heat fluxes (RMSE of 27 Wm^{-2}). The LSP simulation of latent heat flux showed the poorest agreement (RMSE of 122 Wm^{-2}) as compared with the simulation of sensible (RMSE of 29 Wm^{-2}) and ground heat fluxes (RMSE of 5 Wm^{-2}). An investigation of model performance on a typical cloudy day (May 7th) and a typical clear day (May 13th) demonstrated potential for the application of both CLM and LSP in the highly variable climatic conditions of the southeastern US.

CHAPTER 1
INTRODUCTION

Improved quantification of the energy, moisture, and momentum fluxes between the atmosphere and the Earth's surface remains a critical component for studies in hydrology, meteorology and biogeoscience. Scientific endeavors, such as climate modeling, are often interested in quantifying surface fluxes at large spatial scales over a variety of land cover types that are not feasibly monitored using field based techniques. In the stead of complex direct measurement, soil-vegetation-atmosphere transfer (SVAT) models are often used to quantify these fluxes and stores. The most suitable characteristics for SVAT models are often determined by their desired application. The divergence in applications of SVAT models has lead to a variety of models that have structural differences for the characterization of land surface processes. Only by comparing the results of separate SVAT models with a known set of validation data can the utility of different modeling schemes be determined.

The applicability of a given SVAT model is significantly dependent on its required parameterizations and model structure (Schaake et al. 2001). Increased parameterization allows for a greater description of the physical environment and theoretically creates a more robust simulation of surface fluxes. However, this increased robustness often leads to a decreased flexibility in usage. Often a less sophisticated model parameterization can prove advantageous, due to the characteristic heterogeneity of the land surface, as well as a general scarcity of insitu measurement of physical parameters. An effective SVAT

model should incorporate adequate sophistication to accurately simulate the environment, but not be so complex as to reduce usability.

In the Project for Intercomparison of Land surface Parameterization Schemes or PILPS, several scientific teams explored the value of different methods of model parameterization (Pitman and Henderson-Sellers 1998). The multiphase PILPS compared results from as many as 23 land surface models including BATS (Dickinson et al. 1993) and VIC-2L (Liang et al. 1996). The PILPS focus was a community-wide intercomparison of modeling schemes. Thus, none of the studies provided a detailed analysis of individual models. However, the intercomparisons did present results that can be used to guide more detailed intercomparisons (Chen et al. 1997). PILPS Phase 1 comparisons of annually-averaged latent heat flux, sensible heat flux, and radiative temperature, as well as monthly-averaged surface runoff and soil moisture with surface fluxes generated from NCAR climate data showed poor agreement in tropical forest and grassland settings. The revised experimentation framework demonstrated the importance of congruent forcings and parameterization schemes in model comparison studies (Pitman et al. 1999). Phase 2 provided a similar comparison using observed climate data from four different sites, the Cabauw experimental station in the Netherlands (Chen et al. 1997), the HAPEX-MOBILHY site in southwest France (Shao and Henderson-Sellers 1996), the Red-Arkansas River Basin in the Midwestern US (Liang et al. 1998), and a boreal site in Valdai, Russia (Slater et al. 2001). PILPS Phase 2 identified the differences in land surface model mechanisms and characterized the variability in the modeled results. Shao and Henderson-Sellers (1996) describe the difficulty in identifying the link between the model's performance and the responsible mechanism. Because land surface

models are non-linear systems with interacting components, the range of results in each of the Phase 2 intercomparisons is larger than acceptable measurement error. All of the Phase 2 intercomparisons, except those examining snow-covered terrain, exhibited a smaller disparity in latent heat fluxes with respect to the average annual measured latent heat flux than both the sensible heat flux and the ground heat flux (Shao and Henderson-Sellers 1996, Chen et al. 1997, Liang et al. 1998). PILPS demonstrated modeling schemes' strengths in simulating general patterns of land surface processes. The overall scatter in simulation results, which existed between any set of models, may be categorized based on the structure of modeling schemes. However, PILPS's investigation determined that within categories of like modeling schemes there exists varying levels of sensitivity to parameterization (Slater et al. 2001).

While PILPS characterized the overall status of SVATs, model studies that include fewer schemes allow more detailed examination of the models' strengths and weaknesses for a variety of landscapes and climatic conditions. The Mohr et al. (2000) study of the untuned PLACE model in the Southern Great Plains experiment effectively simulated the near surface temperature, moisture and land surface fluxes in the first 48 hours following a heavy rainfall. However, they diverged from observations during the drying period due to simplifications in the parameterization of subsurface moisture, vegetation cover and soil texture. For the prairie grassland in the Radiobrightness Energy Balance Experiment (REBEX) near Sioux Falls, SD, the LSP/R model exhibited small errors when comparing predicted and observed soil and canopy temperatures in a northern prairie over a 14-day period in October (Liou et al. 1999). Energy fluxes were not examined. The van der Keur et al. (2001) study of the modified DAISY SVAT model had good agreement

between the modeled and observed land surface fluxes in non-water limiting conditions for winter wheat in Jutland, Denmark. However, its application during water limiting conditions revealed that the simulated latent heat fluxes underestimated observed values and required a more complete parameterization of canopy resistance during stressed conditions. Nijssen et al. (1997) demonstrated good seasonal agreement with observed fluxes using the hydrology-soil-vegetation model DHSVM in forested sites in the Boreal region of Canada. However, the Nijssen simulation had a time lag for the simulated sensible heat fluxes that suggests the need for a more complete parameterization scheme for the soil thermal model. The importance of SVAT simulation efforts to provide validation in an array of climactic and vegetative conditions is exhibited in the broad range of locations found in existing research: mid-latitude grasslands and croplands (Wood et al. 1998, Liou et al. 1999, Mohr et al. 2000), boreal forests and arctic tundra (Njissen et al. 1997, Kim 1999, Slater et al. 2001), and tropical forests (Pitman et al. 1999). Although SVAT validation research conducted thus far has been representative of several regions and climate types, global extrapolation requires additional validation research across a greater number of climates and biomes.

It is the purpose of this paper to provide a basis for calibration of SVAT modeling processes for the highly variable convective atmospheric conditions and the atypical hydrogeology in the southeastern US. The southeastern US is characterized by subtropical climatic conditions, that consist of high humidity, convective heating and high annual rainfall. The low topographic relief and high water tables create a unique environment for vegetative communities. These communities are distinguished by shallow root zones and variable stomatal resistances and reflectance properties (Mitsch

and Gosselink 2000). A comparison of two SVAT models of contrasting design is used to determine the strengths and weaknesses of each methodology. The Common Land Model (CLM) (Dai et al. 2001) is a regional or watershed scale model, while the Land Surface Process (LSP) model (Liou et al. 1999) is a field scale model. This intercomparison examines the utility of increased sophistication in parameterization as it relates to differences in scale and its practical application in the southeastern US

CHAPTER 2
MODEL COMPARISONS

The Common Land Model (CLM) was developed as part of a multi-disciplinary and multi-institutional project designed to provide land surface forcings for the lower boundary of the Community Climate System Model (Blackmon et al. 2001). Dai et al. (2001) describe the technical elements of CLM. Zeng et al. (2002) and Bonan et al. (2002) demonstrate the coupling of CLM with CCM3. The Land Surface Process (LSP) model is designed to link traditional land surface models and satellite microwave observations to allow for data assimilation (Liou et al. 1999). Judge et al. (2003a and 2003b) describe recent modifications and further developments to the LSP model.

CLM and LSP can be distinguished primarily by their model processes and required parameters that reflect their designed application scale. Table 1 summarizes the differences between their parameterization schemes. As CLM was designed to represent single columns with spatial extents as large as ¼° by ¼°, it incorporates a minimum of insitu measurement of model parameters and initialization data. The only parameters that are user-provided are land cover class, soil texture, longitude, latitude, and soil color index. The remaining environmental parameters are derived from an internal parameterization scheme based on land cover classification. Land cover class is specified based on 18 different International Geosphere-Biosphere Programme (IGBP) classifications (Loveland et al. 2000) from which the remaining vegetation parameters are derived. Estimation of surface fluxes from multiple land cover classifications uses a tile-

mosaic approach similar to Koster et al. (2000). Soil parameters, such as hydraulic conductivity and water retention curves, are generated from empirically based derivations using soil texture (Clapp and Hornberger 1978, Cosby et al. 1984).

Table 1. Methodology for parameterization for CLM and LSP.

Parameters	CLM	LSP
Soil Texture	User Defined	User Defined
η	Empirical Calculation	User Defined
K_{sat}	Clapp and Hornberger	User Defined
λ	Empirical Calculation	User Defined
Wilting Point	User Defined	User Defined
Water Retention Curve	Clapp and Hornberger	User Defined
Root Depth	Empirical Calculation / IGBP	User Defined
LAI	Empirical Calculation / IGBP	User Defined
Canopy Height	IGBP	User Defined
Roughness Length	IGBP	User Defined

In contrast, as LSP was designed as a research tool for field scale applications, it uses a more detailed parameterization scheme and requires insitu measurement of many environmental parameters. Field specific parameters such as soil texture, longitude, latitude, LAI, canopy height, and canopy biomass are user specified. Two physical soil parameters, air entry pressure (Ψ_o) and pore size index (λ), are required to generate the soil water characteristic curve. LSP uses the Rossi and Nimmo (1994) relationship based on the Brooks and Corey water retention model.

The mechanics of the hydrological processes: evapotranspiration, infiltration, and runoff vary significantly between the two models. Table 2 describes these differences for CLM and LSP. Both models determine bare soil evaporation using the Philip and De Vries (1957) diffusion model. CLM's transpiration process is an aerodynamic approach based on the BATS model (Dickinson et al. 1993) with a stomatal resistance component

from the LSM model (Bonan, 1996). LSP's transpiration module uses an aerodynamic approach derived from the CLASS model (Verseghy et al. 1993). LSP's infiltration rate requires soil hydraulic and physical properties, soil temperature, vegetation cover, and surface characteristics like slope and roughness (Ghildyal and Tripathi, 1987). The maximum infiltration rate is estimated using a quasi-analytic solution to Richard's equation for vertical infiltration in a homogeneous soil with a constant initial moisture profile (Green and Ampt, 1911, Philip 1957, Philip 1987a, Philip 1987b).

Table 2. Characterization of land surface processes for CLM and LSP.

Processes	CLM	LSP
Soil Evaporation	Diffusion	Diffusion
Evapotranspiration	Aerodynamic (BATS and LSM based)	Aerodynamic (CLASS based)
Infiltration	Richard's Equation	Richard's Equation (modified)
Subsurface Heat Transport	Fourier's Equation	Fourier's Equation
Runoff	Surface runoff and baseflow (TOPMODEL based)	Hortonian Flow

One of the distinguishing characteristics of CLM is the surface runoff generation process. CLM uses assumptions from the watershed scale model TOPMODEL (Beven et al. 1995) as adapted for land surface modeling (Stieglitz et al. 1997). These assumptions include: a baseflow component defined by the saturated hydraulic conductivity of the lower layers of the profile, an exponential decrease in the saturated hydraulic conductivity with depth and surface runoff based on the parameterization of saturated and unsaturated spatial extents. The exponential decrease of saturated hydraulic conductivity with depth is illustrated in Figure 1 using the conductivities defined by the soil profile used in this study. Figure 1 also illustrates the saturated conductivity used by LSP as parameterized by the soil profile of this study. The parameterization of the fraction of saturated and unsaturated landscape is based on an empirical relationship defined by the relative water table. Since LSP is designed for field scale use only, runoff is only

generated from saturation excess and that depth of water not infiltrated at the end of each timestep.

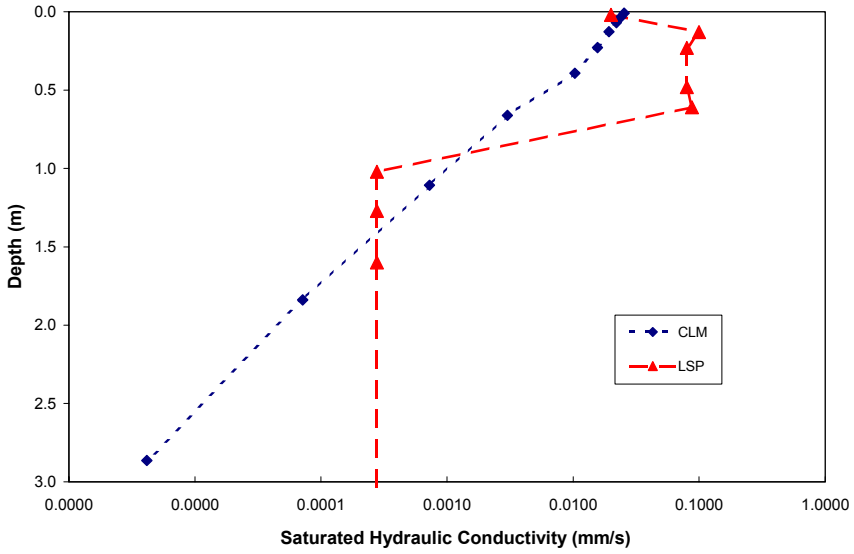

Figure 1. Log scale plot of variation of parameterized saturated hydraulic conductivity with depth below the surface for CLM and LSP

Two modifications were made to CLM. For the low gradient topography and hydrogeology characteristic of much of the southeastern US, the TOPMODEL baseflow generation mechanism is not appropriate. The TOPMODEL baseflow generation mechanism was eliminated allowing the lower layers to remain saturated and eliminating excessive drainage. The parameterization of the relationship between soil moisture and root resistance was also modified for the CLM evapotranspiration mechanism based on measured stresses (Jacobs et al. 2002a).

Both CLM and LSP discretize the soil profile into layers. Each allow soil properties to differ by layer. CLM has a 10-layer profile with the thickness of each layer determined by a unitless scaling factor and an exponential function that increases with depth. Given a typical vertical scaling factor of 0.025, the thickness of the uppermost

layer of CLM is 1.75 cm, while the thickness of the lowest layer is 113.7 cm. LSP layers' thicknesses also increase with depth. However, the LSP profile has 60 layers. The top layers are very fine, yet a deep soil layer may be simulated. Each layer's thickness may be defined as appropriate for the application.

CLM and LSP also have fundamental computational differences. CLM determines the water movement across layer interfaces using a first-order Taylor expansion and solving the resulting equation using a tridiagonal matrix solution. The flux of heat across CLM layer interfaces is solved using the Crank-Nicholson numerical scheme and a tridiagonal matrix solution (Dai et al. 2001). These methods generate soil moisture and temperature profiles at the same temporal resolution as the timestep of the simulation. LSP uses a block-centered finite difference approach that determines the temporal resolution based on the parameterized convergence criteria. The temporal resolution of the resulting LSP profile also differs from the timestep of the climate forcings.

CHAPTER 3
STUDY AREA

The Paynes Prairie State Preserve is a regional basin that contains biological communities such as freshwater marsh, wet prairie and pasture. This 5600 ha system in north-central Florida, USA is 13 km long (east-west) and ranges in the north-south dimension from 1.5 km to 7 km. The summer climate conditions are strongly influenced by surface heating with significant cumulus cloud cover and few cloud-free days. The basin is a large irregularly shaped bowl resulting from solution of the underlying limestone. The basin is either seasonally or perennially flooded based on a surficial aquifer that is separated from the highly transmissive Floridan aquifer by the underlying Hawthorne formation. This geologic formation acts as a semi-confining layer. The primary drain for the Preserve is a sinkhole breach (Alachua Sink) in the semi-confining layer. Based on rainfall patterns, two water-control structures are used to simulate natural basin water levels annually and inter-annually. Generally, water levels are highest during the summer months and lowest during the months of April, September, October, and November. However, no diversion of water into the Preserve through the control structures occurred during the study period due to a multi-year drought.

The study was conducted in a wet prairie community located in the Paynes Prairie Preserve (29^{o} 34' 14 " N, 82^{o} 16' 46 " W). The study period is a 13-day rainless span from May 4^{th} until May 17^{th} of 2001. The study period occurs within a 40-day dry down from saturated conditions from April 17^{th} until May 27^{th}. There is no precipitation during the 40-day dry down period with the exception of three storm events, of which only one

is notable in depth. The first event is a 2.3 cm rainfall on April 27th. The second and third precipitation events are both 0.25 mm in depth and occur on May 2nd and May 17th. As is seen in Figure 2, the water table depth reflects these rainfall patterns. The experiment period is during a steady dry down condition in which the depth to the water table increased from 62 cm to 86 cm.

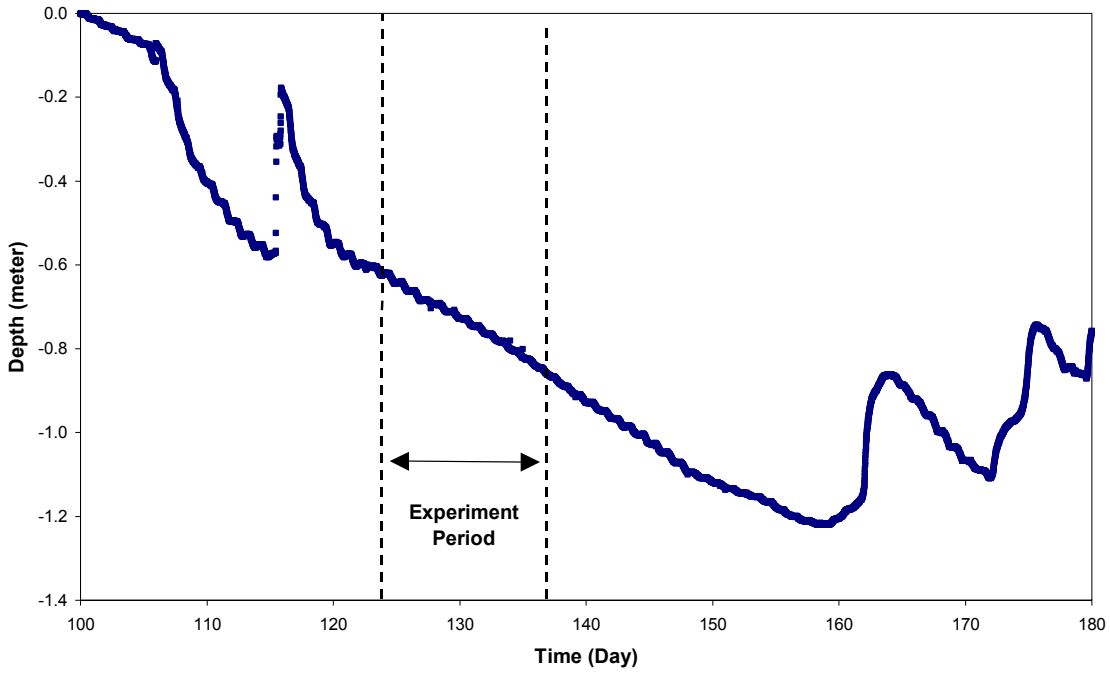

Figure 2. Water table depth with time from April 10th the June 20th. Experiment period from May 4th to May 17th.

The prairie is a relatively flat, treeless plain with moderately dense ground cover. The mean canopy height during the study period is approximately 1.0 m. The site's soils include Emeralda fine sandy loam, Wauberg sand, and Ledwith Muck. The soils consist of sands with an organic surface layer that are underlain by clay. Field observations showed that the majority of the root zone was contained in the upper 10-cm soil layer with approximately 95% of the root zone contained in the upper 25-cm soil layer.

Typically, the wet prairie is inundated for 50 to 100 days each year, burns every two to four years, and has low organic matter acculumulation. This prairie community is routinely burned in accordance with simulated natural periodicity in order to maintain the communities' natural conditions and ecological diversity. Prior to the experiment, the study area was most recently burned in December 1999.

The site is instrumented with a tower-based meteorological station installed onsite to provide several meteorological and micrometeorological measurements. Instrumentation onsite also provided subsurface measurements of water content, soil temperature and soil matric potential. Table 3 describes the instrumentation used for data collection. Jacobs (2002b) also provides a complete description of the instrumentation and study area. All atmospheric and flux instrumentation was mounted on a 6.1-m tower, and logged using a CR10X datalogger (CSI, Inc.). Land surface fluxes were measured using an eddy-flux approach. Evapotranspiration was measured directly using an energy-budget variant of the eddy correlation approach (Tanner and Greene 1989, Twine et al. 2000). Fluctuations in wind speed, virtual air temperature, and vapor density were sampled at 6 Hz, and 30-minute average covariances were calculated to estimate the fluxes. The latent heat fluxes were corrected for temperature-induced fluctuations in air density (Webb et al. 1980) and for the hygrometer sensitivity to oxygen (Tanner and Greene 1989). Sensible heat fluxes were corrected for differences between the sonic temperature and the actual air temperature (Schotanus et al. 1983). Both the sensible and latent heat fluxes were corrected for misalignment with respect to the natural wind coordinate system (Baldocchi et al. 1988). The Bowen-ratio method was used to close the surface energy balance relationship (Twine et al. 2000). Ground heat flux was measured

approximately 10 cm below the surface. The measured soil heat flux was corrected for the energy stored in the upper 10 cm of soil using measurements of soil temperature.

Near-surface volumetric soil water content was recorded at three depths: 7.6 cm, 12.7 cm and 17.8 cm. Soil water potential and soil temperature were also measured within the soil profile at points coinciding with the moisture probe depths, as well as an additional temperature measurements at 2.5 cm. Subsurface measurements were sampled every minute, and 30-minute averages were logged using an AM 416 multiplexer coupled with a CR10X datalogger (CSI, Inc.).

Table 3. Instrumentation used in this study

Variable	Instrumentation	Height (m)
Net Radiation	REBS Q*7.1	6.5
Sensible Heat Flux	CSI 3-D Sonic Anemometer CSAT3	5.75
Latent Heat Flux	CSI Krypton Hygrometer KH20	5.75
Ground Heat Flux	REBS RFT 3.1	-0.1
Wind Speed and Direction	RM Young CS 800-L Anemometer	6.5
Precipitation	Texas Electronincs TE525	6.5
Relative Humidity	Vaisala HMP45c	5.8
Temperature	Vaisala HMP45c	5.8
Pressure	Vaisala PTB100	1.0
Subsurface Temperature	CSI 107	-0.025,-0.076, -0.127, -0.178
Subsurface Moisture	CSI 615L	-0.076, -0.127, -0.179
Subsurface Matric Potential	CSI 257	-0.025,-0.076, -0.127, -0.178

CHAPTER 4
SIMULATION DESIGN

Parameterization

CLM and LSP soil parameters are characterized by soil texture composition from percentages of sand, clay, and loam. The study area's soil is predominantly Wauberg Sand. Parameters for CLM and LSP soil layers were determined by a weighted average based on the soil composition from the Soil Characterization Laboratory soil composition profile (UF-IFAS 1985). Figure 2 illustrates a comparison of the soil water characteristic curves generated from the Clapp and Hornberger relationship used by CLM with soil water characteristic curves derived from measured values. Figure 2 also includes the hydraulic conductivity as it varies with volumetric water content for each of the five CLM layers contained in the top 23 cm of the profile.

Vegetation parameterization for CLM is based on the IGBP characterization of landscapes. The Land Process DAAC (edcdaac.usgs.gov/main.html) defines the study area as a cropland using the IGBP land classification. This characterization, derived from remote sensing data, may be indicative of agricultural pastures bordering the study area, but does not provide an accurate description of the vegetative communities in the region. Due to the hydrogeology and climatic conditions of Paynes Prairie, the plant species within the flooded prairie community are predominately grassland and wetland species. Therefore, the IGBP land cover classification chosen for CLM parameterization was wetland, while within the IGBP parameterization scheme the grassland parameters for leaf and stem reflectance and transmittance were used. CLM's leaf area index (LAI)

parameters are generated from annual maximum and minimum values based on IGBP wetland properties. The temperatures of the lowest soil layer define the seasonal relationship of LAI. LSP's vegetation parameters are user defined. Here, LSP's LAI was proportionally increased during the experiment from 2.0 to 2.5,

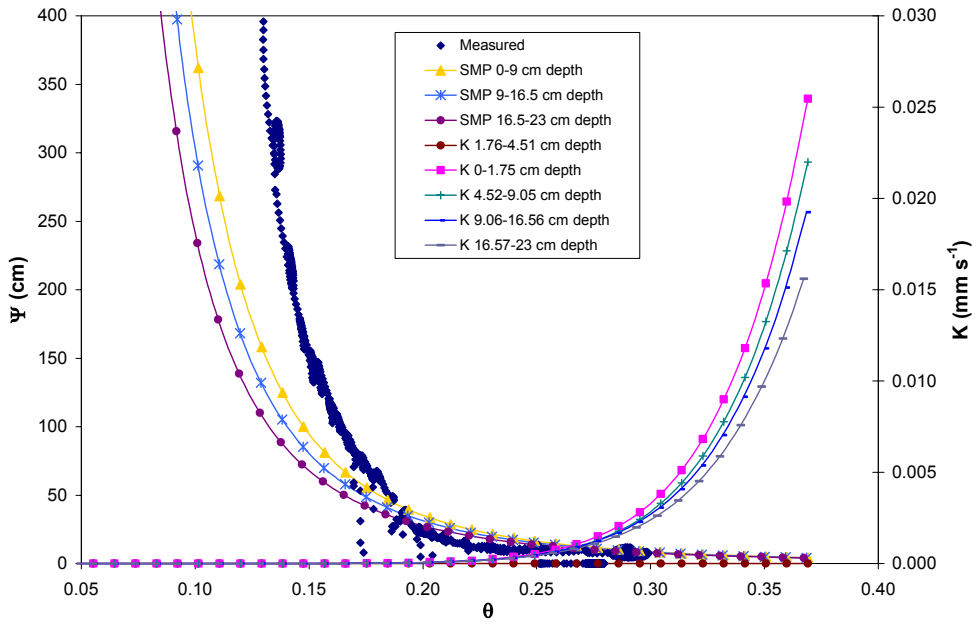

Figure 3. Comparison of measured soil water characteristic curve with three soil water characteristic curves defined by modeled soil matric potential (SMP) and seven hydraulic conductivity (K) curves based on the Clapp and Hornberger relationship within the CLM parameterization scheme.

Initialization

The CLM and LSP initialization schemes require the initial soil temperature profile and the initial soil moisture content profile. The soil temperature profile is intialized using measured values for the top 23 cm. For the lower profile, the initial temperature is set equal to the temperature measured at 23 cm. The soil moisture profile is initialized using measurements in the top 17 cm of the profile. The profile is saturated below 62 cm. The initial soil moisture is assumed to increase linearly with depth between 17 cm and the water table.

Forcings

Table 4 summarizes the forcings required by CLM and LSP. All forcings excluding radiation, are from measured values. Estimates of incoming shortwave and longwave radiation were derived from measured net radiation. During the nighttime (generally 6:30 PM to 6:30 AM EDT), shortwave radiation is zero and net longwave radiation is equivalent to measured net radiation. Daytime values of the longwave radiation balance were estimated using Diak et al.'s (2000) remotely-sensed radiation estimation scheme based on GOES data. Jacobs et al. (2002b) demonstrated the utility of GOES data in the study area. The diurnal radiation surface albedo as a function of time was determined for a cloud-free day using measured incoming shortwave radiation, measured net radiation and GOES estimated net longwave. The solar insolation is calculated from measured net radiation, GOES derived net longwave radiation and surface albedo.

Table 4. Required atmospheric forcings for CLM and LSP

Model Forcings	
CLM	LSP
Incoming Shortwave Radiation (Wm^{-2})	Incoming Shortwave Radiation (Wm^{-2})
Incoming Longwave Radiation (Wm^{-2})	Incoming Longwave Radiation (Wm^{-2})
Air Temperature (K)	Air Temperature (K)
Specific Humidity (-)	Relative Humidity (%)
Precipitation (mm $0.5hr^{-1}$)	Precipitation (mm $0.5hr^{-1}$)
Wind Speed (ms^{-1})	Wind Speed (ms^{-1})
Atmospheric Pressure (hPa)	

CHAPTER 5
RESULTS AND DISCUSSION

The CLM and LSP simulation results are evaluated using three categories. The modeled soil moisture, soil temperature and surface heat fluxes are compared with measured validation data. The two main statistical quantities used for simulation assessment are mean absolute error (MAE) and root mean squared error (RMSE). The mean absolute error is defined as the average of the absolute differences between modeled and measured results:

$$\mathrm{MAE} = \frac{\sum_{i=1}^{n} \left| X_{\mathrm{mod},i} - X_{\mathrm{meas},i} \right|}{n}$$

Equation 1. Mean absolute error.

The root mean squared error is the square root of the average of the differences between modeled and measured results squared, as follows:

$$\mathrm{RMSE} = \sqrt{\frac{\sum_{i=1}^{n} \left(X_{\mathrm{mod},i} - X_{\mathrm{meas},i} \right)^2}{n}}$$

Equation 2. Root mean squared error.

Soil Moisture

The observed point measurements of soil moisture were compared to the simulated moisture for the layer that contains that measurement point. Each CLM and LSP soil

layer has homogeneous moisture and temperature. The soil moisture measurements at 7.6, 12.7 and 17.8 cm correspond to CLM layers 3, 4 and 5, respectively and to LSP layers 11, 15 and 19. Figure 3 shows the evolution of modeled and measured soil moisture during the study period in terms of volumetric water content (VWC).

CLM's layer 3 exhibits a more rapid dry down than the observed dry down. This layer has a higher modeled water content than observed during the first two days of the experiment. The model dry down rate results in the simulated layer having a lower moisture content than the observed for all periods after four days with an increasing bias for the duration. The MAE and RMSE for the CLM simulated results are 0.013 m^3m^{-3} and 0.016 m^3m^{-3}. LSP matches the dry down rate of the measurement at 7.6 cm, however, there is an initial offset in the modeled results of approximately 0.03 m^3m^{-3}. This initial offset results in a high bias of simulated moisture contents for the entire experimental period. The LSP simulated results demonstrate a MAE and RMSE of 0.034 m^3m^{-3} and 0.035 m^3m^{-3}.

The CLM simulation results corresponding to the 12.7 cm measurement demonstrate good agreement with the measured dry down rate. A small bias results in simulated moisture content values that are lower than measured by approximately 0.03 m^3m^{-3} throughout the study period. The LSP model shows very good agreement with the measured values over the period. The MAE and RMSE for the LSP modeled results are 0.009 m^3m^{-3} and 0.011 m^3m^{-3}. Both CLM and LSP show a similar rate of dry down for the measurements at 12.7 and 17.8 cm and provide good moisture content estimates at the deepest measurement depth. CLM's moisture contents are slightly drier (0.01 m^3m^{-3}) than measured, while LSP's modeled water contents are slightly wetter (0.02 m^3m^{-3}).

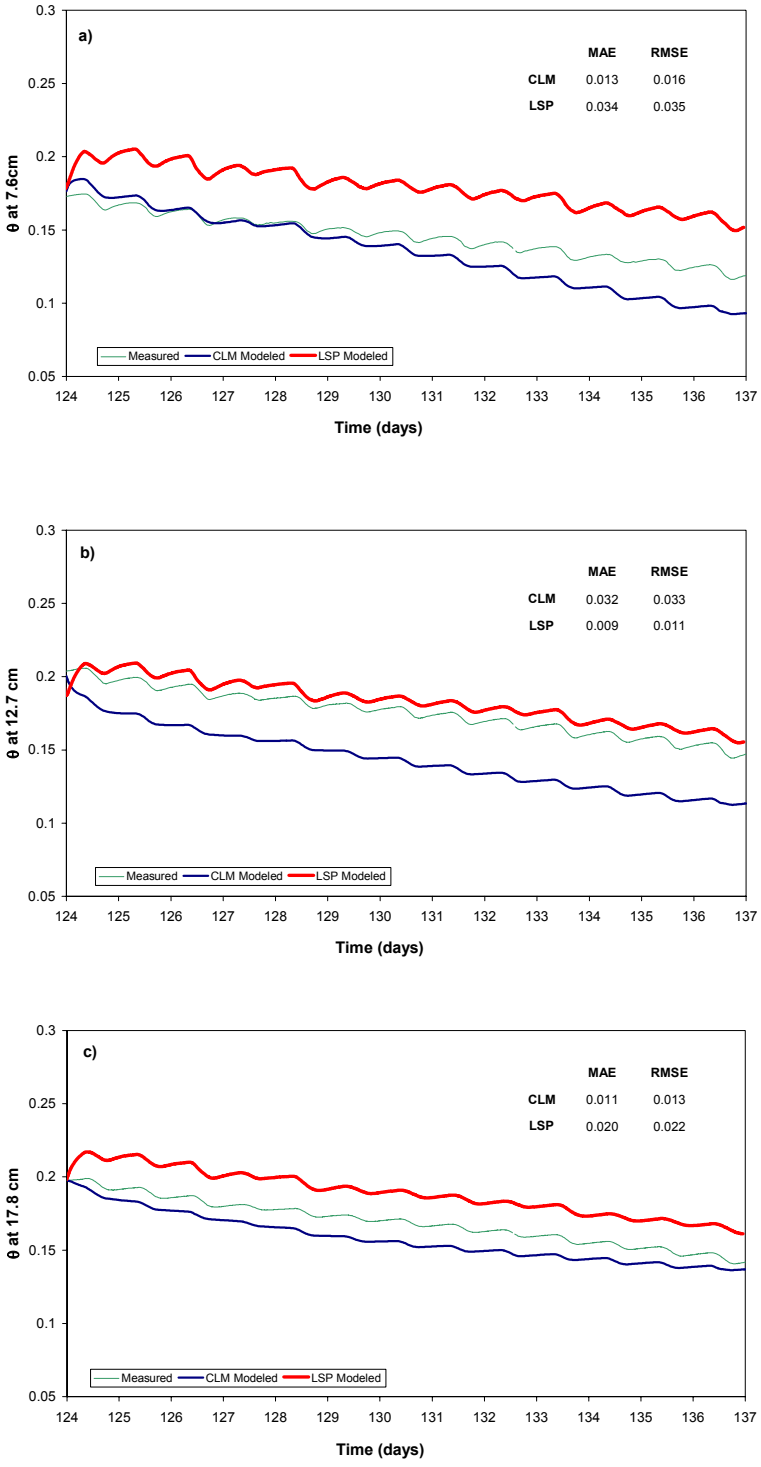

Figure 4. Comparison of measured soil moisture with CLM and LSP modeled soil moisture at a) 7.6 cm, b) 12.7 cm and c) 17.8 cm.

The measurement error associated with a CS615 moisture probe is ± 2.5% volumetric water content. CLM simulations at 7.6 and 17.8 cm depths have errors less than the instrument error. The CLM simulation at 12.7 cm is less than 1.5 times the instrument error. LSP's 7.6 cm depth exhibits error of less than 1.5 times the instrument error. LSP's 12.7 cm and 17.8 cm depths show better agreement with an error less than the instrument error. The volumetric soil moisture errors identified in this study are consistent with the results of other studies. In PILPS Phase 2(b), Shao and Henderson-Sellers (1996) recognized ±3% volumetric water content error margins as reasonable, while Mohr et al. (2000) found error margins in the near surface soil simulation of ±5% volumetric soil moisture.

Comparisons of the modeled results to the observations suggest different strengths and weaknesses for each model. For all three depths, both models capture the diurnal fluctuations in moisture. The observations showed increasing soil moisture as the soil water profile reestablished during the evening. LSP did an excellent job of modeling the phase and amplitude of the measured soil moisture fluctuations throughout the experiment period. Both are able to capture the magnitude and location of soil water extraction due to evapotranspiration. While, CLM's daytime dry down appears to function appropriately, CLM was unable to replicate the recharge from the lower layers.

The water retention curves used by the models appear to result in two distinct errors. For LSP, the soil water profile rapidly equilibriates to a biased profile. The LSP soil water retention curve appears shifted such that the soil matric potential for each depth corresponds to a higher moisture content than the moisture content that is measured. CLM overestimates the daily dry down rate, because it does not redistribute water from

lower layers to upper layers during the nighttime. This pattern can be explained by examining the CLM soil water characteristic curves in Figure 2. For soil moisture contents between 0.15 m^3m^{-3} and 0.17 m^3m^{-3}, the slope of the measured retention curve is very steep, however, the CLM water retention curve is relatively flat in this range. Daytime root water extraction results in an observed soil water profile that increases in depth from the surface. This profile results in a large gradient of matric potentials in response to the moisture content profile that drives soil water upward in the soil profile during the evening. However, in CLM's modeled soil column, comparable moisture profiles exhibit a much smaller gradient of matric potential. Thus, CLM has a reduced upward movement of moisture and increasingly dryer surface conditions.

Soil Temperature

The comparison of the modeled soil temperature profile with observed soil temperatures follows that methodology for the soil moisture comparison. Soil temperature and moisture were measured at the same depths with an additional temperature measurement at 2.5 cm depth. The time evolution of modeled CLM and LSP soil temperatures compared with measured values for the observation period are seen in Figure 4. Overall, both models show good agreement with the timing and magnitude of the actual diurnal fluctuations. Simulated soil temperatures of both CLM and LSP for all depths show a warming trend over the study period. For the 2.5 cm depth, the maximum daily soil temperature increases by 2 K over the two-week period. However, the simulated maxima are somewhat warmer than the measured maximum during the latter parts of the experiment. For the second depth, the maxima of both simulations are within 1 K of the measured maximum early in the experiment and greater than 3.0 K and 2.0 K for CLM and LSP, respectively, at the end of the experiment. At the 7.6 cm

measurement depth, both simulations lead the measured diurnal fluctuations by 2.0 to 3.0 hours throughout the study period. While the temperatures are quite similar, the shift increases in errors to 1.2 K and 1.4 K for CLM and 0.8 K and 0.98 K for LSP. The 12.7 and 17.8 cm comparisons do not have a temporal discrepancy. Both comparisons exhibit the same enhanced warming trend that is evident at both 2.5 and 7.6 cm, as shown in Figures 4 c and d. At 12.7 cm, the early diurnal cycles show slightly lower modeled temperature maxima than the measured temperature maximum. The agreement improves during the experimental period with the final diurnal cycle exhibiting good agreement as compared to the measurements. The MAE and RMSE are 0.45 K and 0.54 K for CLM and 0.52 K and 0.67 K for LSP. The 17.8 cm measurements compare well with both simulated time series for the first 10 days with the final three cycles showing a small warm bias of 1.5 K between the measured and modeled temperatures at all points during the cycle. The lowest layer had the smallest error for both CLM with a MAE and RMSE of 0.35 K and 0.44 K and LSP with errors of 0.33 K and 0.41 K.

For both models, the modeled error decreases with depth, as the diurnal fluctuations are damped by the increasing soil thickness. The measurement error associated with a CS107 temperature probe is ± 0.5 K. Analysis of the CLM modeled soil temperatures shows an agreement with the 2.5 cm and 7.6 cm measured values within 2.5 times the instrument error. The comparison of the CLM modeled temperatures with the 12.7 cm and the 17.8 cm measured values show errors less than the instrument error. The LSP simulation shows a similar trend. From the 2.5 to 17.8 cm depths, the ratio of LSP's MAE's compared to the instrument errors are less than 2.5, 2.0, 1.5 and 1.0, respectively. The errors of the simulated soil temperatures compare reasonably

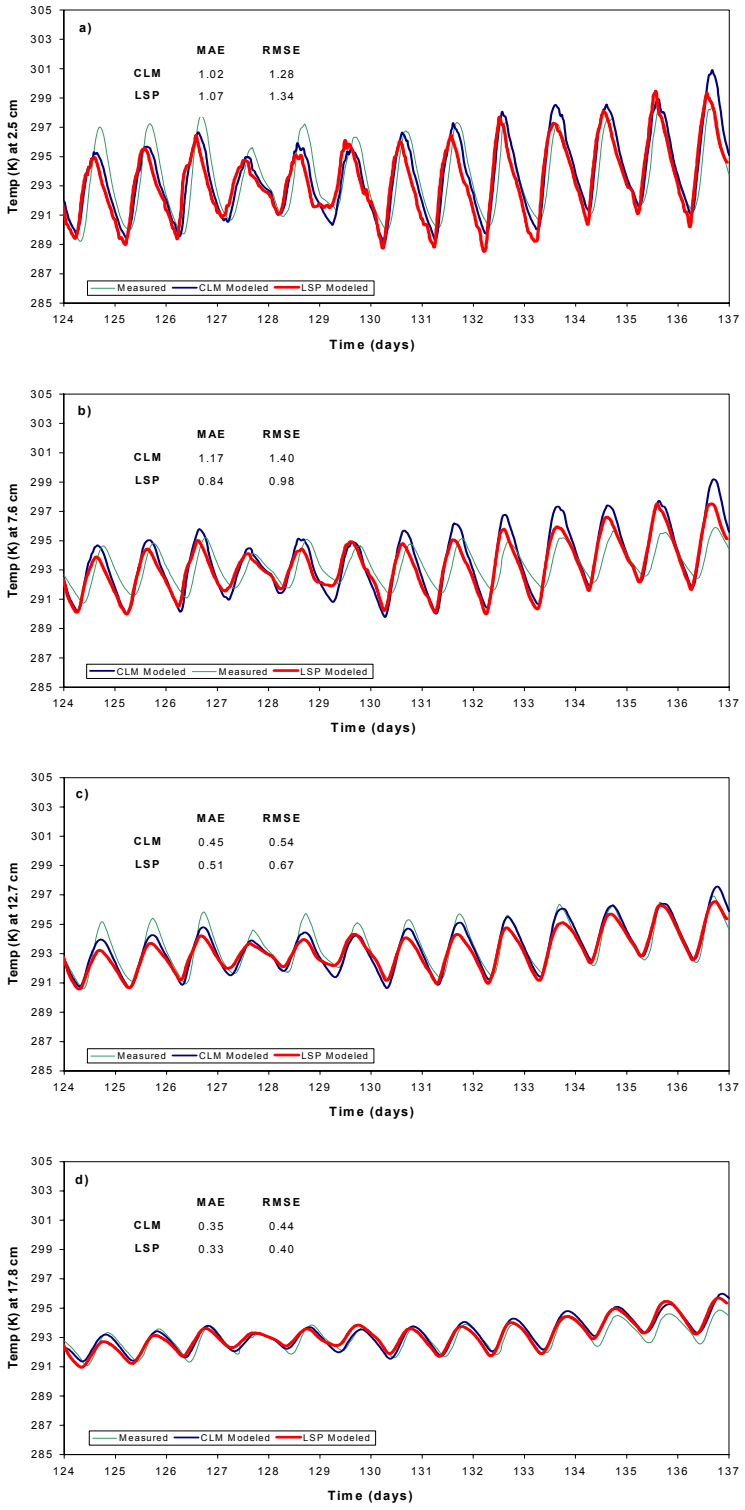

Figure 5. Comparison of measured subsurface soil temperature and CLM and LSP modeled soil temperature at a) 2.5 cm, b) 7.6 cm, c) 12.7 cm and d) 17.8 cm.

well with similar modeling studies. Both Chen et al. (1997) and Mohr et al. (2000) found errors within ±2 K for subsurface temperatures. The offline simulations of PILPS Phase 1 found ranges between models of 1.4 K for tropical forest and 2.2 K for grassland in a multi-year study. Judge et al. (2003b) found a 1.8 K average difference between modeled and measured temperature for bare soil and a 1.0 K mean difference for brome grass.

In general, the modeled temperatures for both models show a warming trend over the duration of the period at all depths. This trend reflects the observed dry down and warming conditions. CLM's simulated diurnal temperature fluctuations are greater in magnitude than LSP's. This likely reflects the decreased thermal heat capacity of CLM's relatively drier soil. Despite the higher moisture content, the LSP layers' temperatures generally show higher fluctuations in temperature than the measurements. This could be due to the soil texture parameterized thermal capacity of dry soil within LSP being lower than the actual thermal capacity of the soil solids.

Surface Heat Fluxes

The comparison of modeled surface fluxes with observations from field data demonstrates some disparity in the modeled energy balance for both models. Figure 5a demonstrates the agreement of CLM modeled net radiation and measured net radiation. As both downwelling longwave and shortwave radiation force CLM, the agreement of the net radiation demonstrates the accuracy of the simulated reflected radiation or albedo and upwelling longwave radiation. Figures 5b, 6a and 6b illustrate the differences between the observed fluxes and the CLM and LSP modeled fluxes for three components of the energy balance: latent heat flux, sensible heat flux and ground heat flux. The ground heat flux of CLM is compared to the measured ground heat flux at the surface (10 cm depth measurement corrected for soil heat storage), while the LSP ground heat flux

for model layer 13 is comparable to the actual 10 cm flux measurement (Figure 6b). The MAE and RMSE were calculated using only daytime values (6:30 am until 6:30 pm) due to missing nighttime measurements resultant from dew on the lens of the krypton hygrometer.

The CLM results for latent heat fluxes show the best agreement, while the sensible heat and ground heat fluxes have larger errors. The LSP results have the largest discrepancy between simulated and measured fluxes for latent heat fluxes, whereas the sensible heat and ground heat fluxes demonstrate better agreement. The diurnal variation in all energy fluxes is well captured by both models, with the exception of the LSP latent heat flux. The diurnal variation of the simulated latent heat flux increasingly lags the measured diurnal variation as the experimental period progresses. At the beginning of the experiment, the diurnal variation of the simulated latent heat fluxes lags the measured by 2 hrs. The lag is approximately 3 hrs during the last day of the experiment. The MAE and RMSE derived from comparisons of the measured and modeled latent heat for CLM is 44.79 Wm^{-2} and 61.69 Wm^{-2}. The corresponding statistics for the LSP simulation are 99.43 Wm^{-2} and 122.32 Wm^{-2}. A MAE of 47.09 Wm^{-2} and a RMSE of 60.92 Wm^{-2} is derived from comparisons of the measured and CLM simulated sensible heat flux. LSP has much better agreement with measured sensible heat flux with respective MAE and RMSE values of 23.50 Wm^{-2} and 29.08 Wm^{-2}. CLM has relatively high errors of 20.83 Wm^{-2} and 26.19 Wm^{-2} for the MAE and RMSE of the simulated ground heat flux as compared to LSP's errors of 4.27 Wm^{-2} and 5.31 Wm^{-2}.

The MAE associated with the simulated daytime CLM latent heat flux represents 19% of the average 232.11 Wm^{-2} measured latent heat flux. The MAE of the LSP

simulation is 43% of the average measured latent heat. The magnitude of the CLM daytime sensible heat MAE is approximately 48% of the magnitude of the average measured sensible heat flux, 98.7 Wm^{-2}. A similar examination of LSP shows the magnitude equal to approximately 24% of the average measured sensible heat flux. The MAE resulting from comparisons of the measured and CLM daytime simulated ground heat flux is nearly equal to the average magnitude of the measured ground heat flux of 22.55 Wm^{-2} representing approximately 92% of the magnitude. The MAE of LSP daytime simulated ground heat flux is only 19% of the average measurement magnitude.

Simulation of surface fluxes often provides the largest discrepancies from measurements. Chen et al. (1997) found reasonable agreement with ranges across modeling schemes of 30 Wm^{-2} and 25 Wm^{-2} for sensible and latent heat flux, respectively. Chang et al. (1999) also found good agreement using the CAPS model, with a monthly discrepancy of 7.1 Wm^{-2} in latent heat flux and 7.7 Wm^{-2} for sensible heat flux. However the same study found discrepancies in diurnal amplitude of ground heat flux around 20 Wm^{-2} with a phase difference of 2.5 hours. Both Chen et al. (1997) and Chang et al. (1999) calculated error margins based on the full diurnal cycle. A trend evident in several SVAT model validation studies (Acs and Hantel 1998, Chang et al. 1999, Gonzalez-Sosa et al. 2001) is that latent heat fluxes are more accurately simulated than sensible heat fluxes and ground heat fluxes. This trend suggests that the model physics representing the processes of latent heat flux are more comprehensive than the model physics describing the sensible or ground heat flux. The results of the CLM simulation provide another example of this tendency. In contrast, the LSP model has a tendency to underpredict the latent heat fluxes as the soil column dries out and

evapotranspiration conditions drop below potential, while accurately simulating the sensible and ground heat fluxes.

As the climatic conditions of the southeastern US may significantly influence model performance, a comparison of modeled fluxes were examined for two days that exhibit large differences in cloud cover. Within the experimental period, May 7th represents a typical cloudy day, whereas May 13th is a typical clear-sky day. The average measured net radiation is 210.4 Wm^{-2} on May 7th and 394.2 Wm^{-2} on May 13th. Figures 7 a, b and c illustrate the latent heat flux, sensible heat flux and ground heat fluxes for May 7th. Both CLM and LSP underpredict the latent heat fluxes during the first 5.0 hours of the cloudy diurnal cycle. In order to maintain the energy balance, both CLM and LSP overpredict the measured sensible heat during the same period. CLM also overpredicts ground heat fluxes for the first half of the day, while LSP shows very good agreement throughout the day. During midday, the net radiation shows high variability that is indicative of cumulus atmospheric conditions. CLM closely tracks the variation in net radiation, but overpredicts the effect of that variability on the measured latent and sensible heat fluxes. While LSP demonstrates similar patterns, LSP better captures the effect of the variability. This may be a function of LSP's higher temporal resolution of the simulation.

Figures 8 a, b and c demonstrate the latent heat, sensible heat and ground heat fluxes for the relatively clear skies observed on May 13th. CLM's simulated latent heat fluxes underpredict measured latent heat fluxes for the first three hours of the diurnal cycle. After the initial period, the measured values are overpredicted until the peak. CLM's latent heat and sensible heat fluxes show similar agreement with the

measurements. Whereas the modeled latent heat fluxes overpredict midday values, the modeled sensible heat fluxes underpredict during the same period. LSP's simulated latent heat fluxes underpredict the measured latent heat fluxes for the first 10 hours of the day. The diurnal variation of LSP's simulated latent heat fluxes has a 3 hr phase shift. LSP's simulated sensible heat and ground heat fluxes show very good agreement with the measured fluxes over the course of the day. Overall, both models seem to simulate the surface energy fluxes well in both clear sky and convective climatic conditions. These results support the validity of the CLM and LSP model physics for determination of high temporal resolution applications for climates typical of the southeastern US.

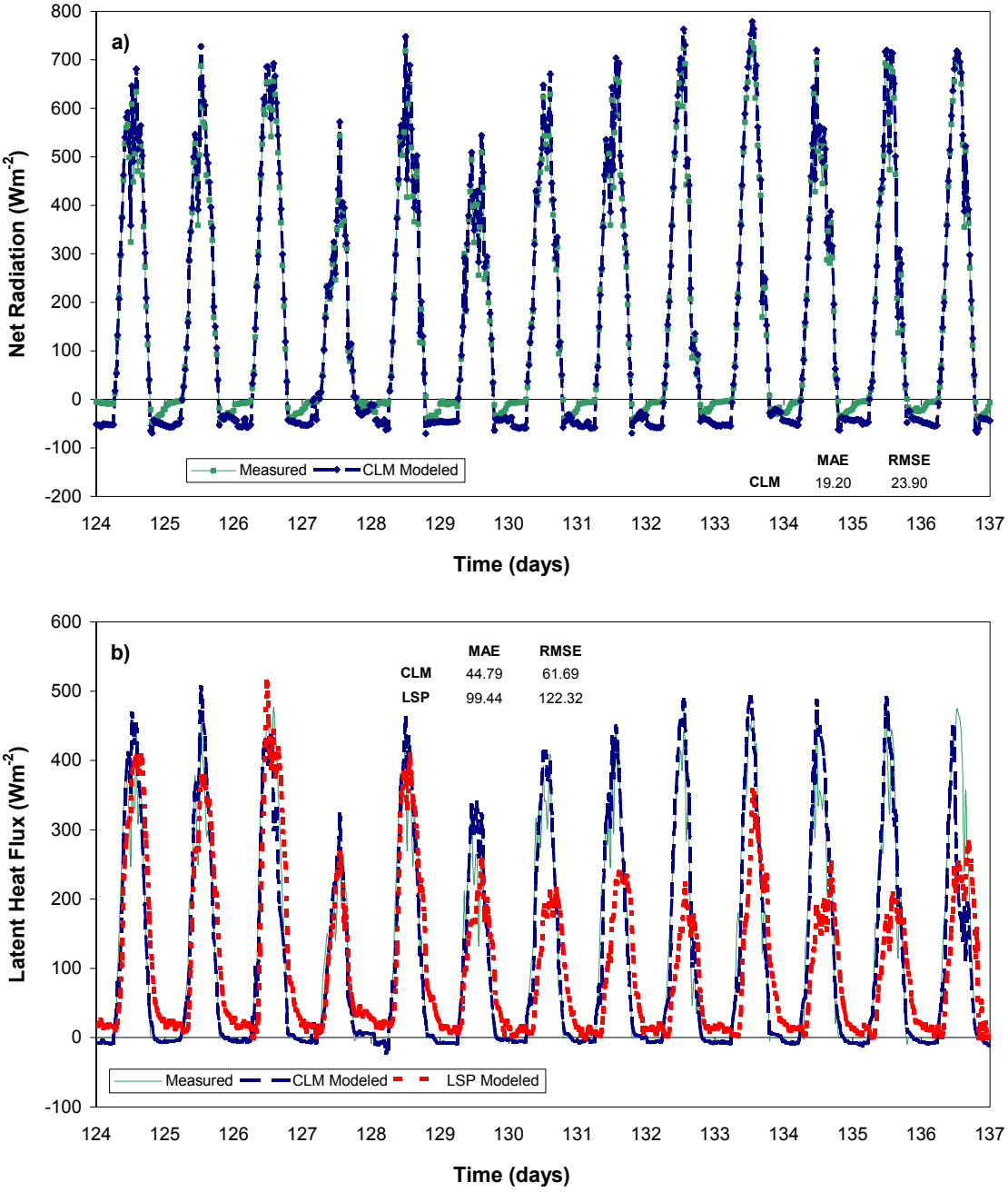

Figure 6. Comparison of modeled and measured surface fluxes for a) CLM net radiation and b) CLM and LSP latent heat flux.

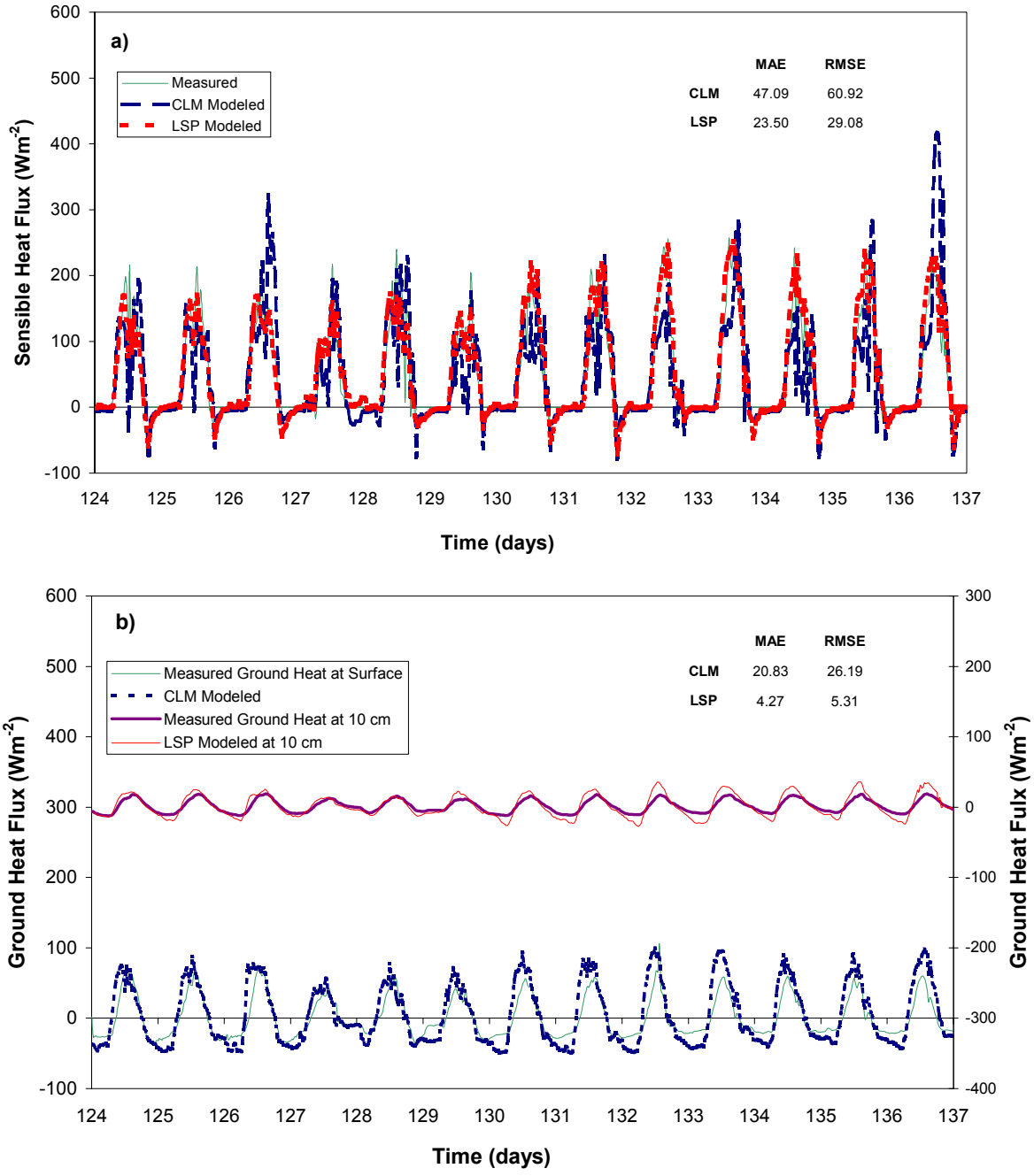

Figure 7. Comparison of modeled and measured surface fluxes for a) CLM and LSP sensible heat flux and b) CLM and LSP ground heat flux.

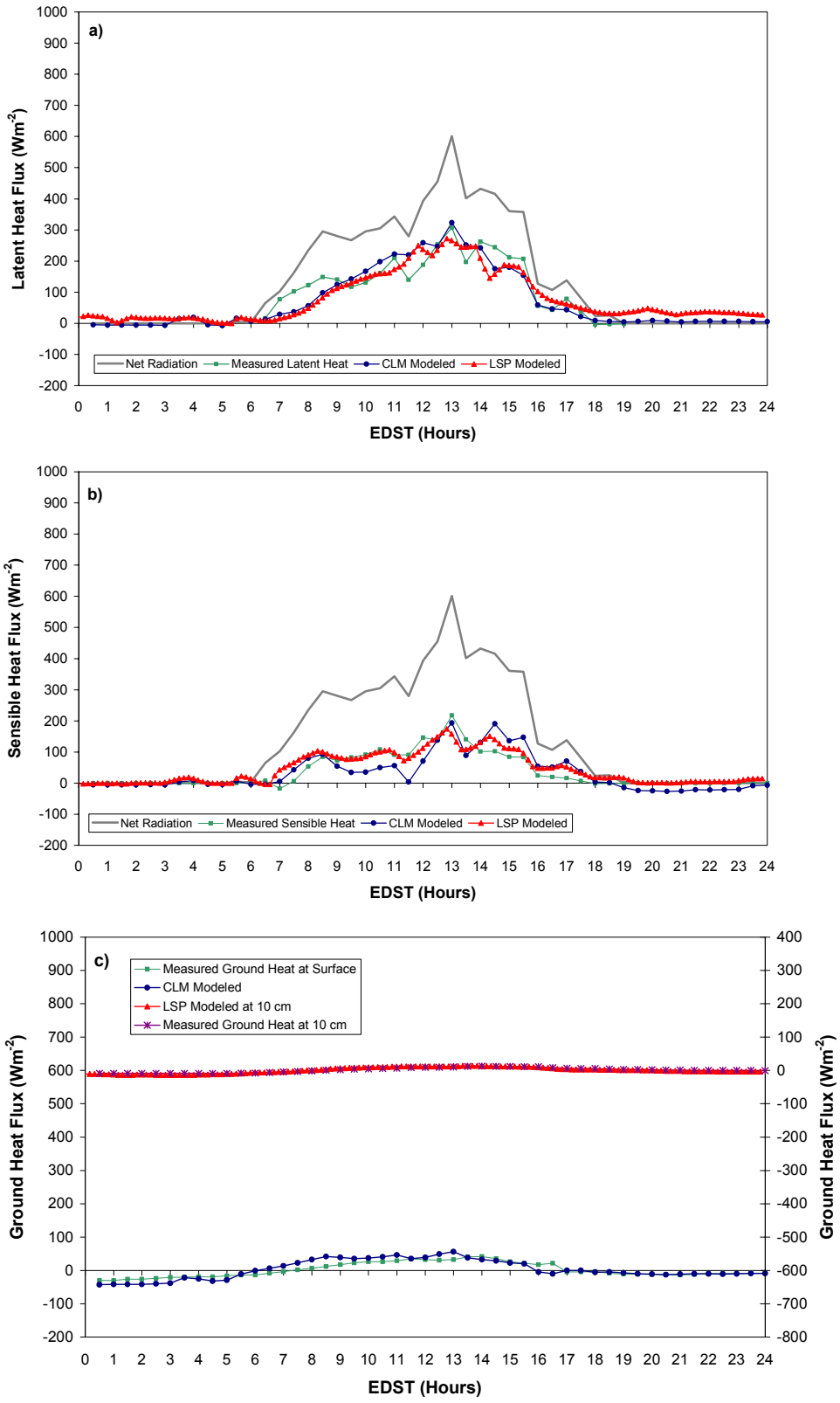

Figure 8. Comparison of measured and modeled surface energy fluxes for a typical cloudy day, May 7th for a) Latent heat flux, b) Sensible heat flux and c) Ground heat fluxes.

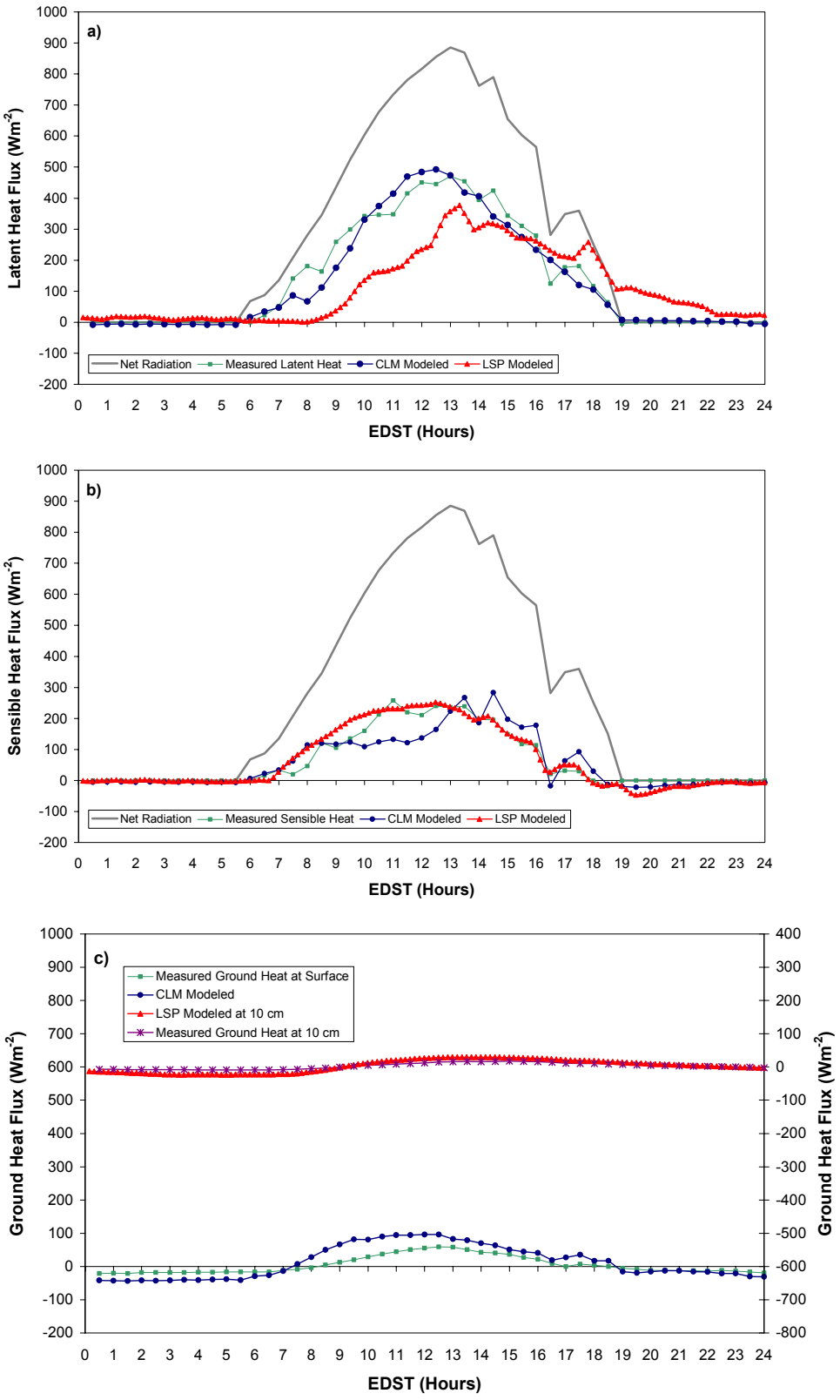

Figure 9. Comparison of measured and modeled surface energy fluxes for a typical clear day, May 13th for a) Latent heat flux, b) Sensible heat flux and c) Ground heat fluxes.

CHAPTER 6
CONCLUSION

The purpose of this research was to compare two SVAT models' applicability in a high water table environment characteristic of the southeastern US. As all SVAT models rely on similar mathematical approximations of biophysical reality, the main difference between a field scale model and a watershed scale single-column model is parameterization. LSP's strength is its meticulous reproduction of biophysical mechanisms at the land surface. In order to provide an exhaustive simulation of land surface processes, the LSP model can use all available data to parameterize the canopy and soil profile. Alternatively, CLM has an inherent database that contains default parameterization schemes for each IGBP land cover.

The results indicate that both CLM and LSP can be used with success in the convective climate and high water table environment of the southeastern US. The two models were used to simulate a 13-day dry drown. The simulations show that subsurface moisture content and surface energy fluxes provide good agreement with measured values. Both models' simulated soil temperatures show very good agreement as compared to measured temperatures. The models were able to appropriately replicate the soil warming that occurred over the experimental period as well as the diurnal fluctuations. Both models simulated energy fluxes within expected error ranges. When considering the field scale of the experiment, CLM performs quite well in comparison with the biophysically more sophisticated LSP model. However, for use in the southeastern US, it is important to alter CLM's baseflow generation physics mechanism

to account for the low relief topography of the region. Overall, the experiment demonstrates potential for the application of both CLM and LSP in the southeastern US.

LIST OF REFERENCES

Acs, F. and M. Hantel, 1998: The land-surface flux model PROGSURF. *Global and Planetary Change*, **19,** 19-34.

Baldocchi, D. D., B. B. Hicks, and T. P. Meyers, 1988: Measuring Biosphere-Atmosphere Exchanges of Biologically Related Gases with Micrometeorological Methods. *Ecology*, **69,** 1331-1340.

Beven, K. J., R. Lamb, P. Quinn, R. Romanowicz, and J. Freer, 1995: Topmodel. *Computer Models of Watershed Hydrology*, Water Resource Publications, Highlands Ranch, CO, 627-668.

Blackmon, M., B. Boville, F. Bryan, R. Dickinson, P. Gent, J. Kiehl, R. Moritz, D. Randall, J. Shukla, S. Solomon, G. Bonan, S. Doney, I. Fung, J. Hack, E. Hunke, J. Hurrell, J. Kutzbach, J. Meehl, B. Otto-Bliesner, R. Saravanan, E. K. Schneider, L. Sloan, M. Spall, K. Taylor, J. Tribbia, and W. Washington, 2001: The Community Climate System Model. *Bulletin of the American Meteorological Society*, **82,** 2357-2376.

Bonan, G. B., 1996: A land surface model (LSM version 1.0) for ecological, hydrological, and atmospheric studies: Technical Description and User's Guide. *NCAR Technical Note*, **NCAR/TN-417+STR,** 150.

Bonan, G. B., K. W. Oleson, M. Vertenstein, S. Levis, X. B. Zeng, Y. J. Dai, R. E. Dickinson, and Z. L. Yang, 2002: The land surface climatology of the community land model coupled to the NCAR community climate model. *Journal of Climate*, **15,** 3123-3149.

Chang, S., D. Hahn, C. H. Yang, and D. Norquist, 1999: Validation study of the CAPS model land surface scheme using the 1987 Cabauw/PILPS dataset. *Journal of Applied Meteorology*, **38,** 405-422.

Chen, T. H., A. HendersonSellers, P. C. D. Milly, A. J. Pitman, A. C. M. Beljaars, J. Polcher, F. Abramopoulos, A. Boone, S. Chang, F. Chen, Y. Dai, C. E. Desborough, R. E. Dickinson, L. Dumenil, M. Ek, J. R. Garratt, N. Gedney, Y. M. Gusev, J. Kim, R. Koster, E. A. Kowalczyk, K. Laval, J. Lean, D. Lettenmaier, X. Liang, J. F. Mahfouf, H. T. Mengelkamp, K. Mitchell, O. N. Nasonova, J. Noilhan, A. Robock, C. Rosenzweig, J. Schaake, C. A. Schlosser, J. P. Schulz, Y. Shao, A. B. Shmakin, D. L. Verseghy, P. Wetzel, E. F. Wood, Y. Xue, Z. L. Yang, and Q. Zeng, 1997: Cabauw experimental results from the project for intercomparison of land-surface parameterization schemes. *Journal of Climate*, **10,** 1194-1215.

Clapp, R. B. and G. M. Hornberger, 1978: Empirical Equations for Some Soil Hydraulic-Properties. *Water Resources Research*, **14,** 601-604.

Cosby, B. J., G. M. Hornberger, R. B. Clapp, and T. R. Ginn, 1984: A Statistical Exploration of the Relationships of Soil-Moisture Characteristics to the Physical-Properties of Soils. *Water Resources Research*, **20,** 682-690.

Dai, Y., X. Zeng, and R. Dickinson, 2001: Common Land Model (CLM): Technical Documentation and User's Guide. (climate.eas.gatech.edu/dai/clmdoc.pdf), 69.

Diak, G. R., W. L. Bland, J. R. Mecikalski, and M. C. Anderson, 2000: Satellite-based estimates of longwave radiation for agricultural applications. *Agricultural and Forest Meteorology*, **103,** 349-355.

Dickinson, R., A. Henderson-Sellers, P. J. Kennedy, and M. F. Wilson, 1993: Biosphere atmosphere transfer scheme (BATS) version 1e as coupled to the NCAR Community Climate Model. *NCAR Technical Note*, **NCAR/TN-378+STR,** 72.

Ghildyal, B. P. and R. Tripathi, 1987: *Soil Physics*. New York City, NY, John Wiley.

Gonzalez-Sosa, E., I. Braud, J. L. Thony, M. Vauclin, and J. C. Calvet, 2001: Heat and water exchanges of fallow land covered with a plant- residue mulch layer: a modelling study using the three year MUREX data set. *Journal of Hydrology*, **244,** 119-136.

Green, W. and G. Ampt, 1911: Studies on soil physics. *Journal of Agricultural Science*, **4,** 1-24.

Jacobs, J. M., D. A. Myers, M. C. Anderson, and G. R. Diak, 2002a: GOES surface insolation to estimate wetlands evapotranspiration. *Journal of Hydrology*, **266,** 53-65.

Jacobs, J. M., S. L. Mergelsberg, A. F. Lopera, and D. A. Myers, 2002b: Evapotranspiration from a wet prairie wetland under drought conditions: Paynes Prairie Preserve, Florida, USA. *Wetlands*, **22,** 374-385.

Judge, J., L. M. Abriola, and A. W. England, 2003a: A summertime Land Surface Process and Radiobrightness model - Part I: Development and Numerical Validation. *Advances in Water Resources***,** in review.

Judge, J., J. Metcalfe, D. McNichol, B. E. Goodison, A. E. Walker, and A. W. England, 2003b: A summertime Land Surface Process and Radiobrightness model - Part II: Model Calibration. *Water Resources Research***,** in review.

Kim, E. J., 1999: Remote sensing of land surface conditions in arctic tundra regions for climatological applications using microwave radiometry, PhD thesis, University of Michigan.

Koster, R. D., M. J. Suarez, A. Ducharne, M. Stieglitz, and P. Kumar, 2000: A catchment-based approach to modeling land surface processes in a general circulation model 1. Model structure. *Journal of Geophysical Research-Atmospheres*, **105,** 24809-24822.

Liang, X., D. P. Lettenmaier, E. F. Wood, and S. J. Burges, 1994: A Simple Hydrologically Based Model of Land-Surface Water and Energy Fluxes for General-Circulation Models. *Journal of Geophysical Research-Atmospheres*, **99,** 14415-14428.

Liang, X., E. F. Wood, and D. P. Lettenmaier, 1996: Surface soil moisture parameterization of the VIC-2L model: Evaluation and modification. *Global and Planetary Change*, **13,** 195-206.

Liang, X., E. F. Wood, D. P. Lettenmaier, D. Lohmann, A. Boone, S. Chang, F. Chen, Y. J. Dai, C. Desborough, R. E. Dickinson, Q. Y. Duan, M. Ek, Y. M. Gusev, F. Habets, P. Irannejad, R. Koster, K. E. Mitchell, O. N. Nasonova, J. Noilhan, J. Schaake, A. Schlosser, Y. P. Shao, A. B. Shmakin, D. Verseghy, K. Warrach, P. Wetzel, Y. K. Xue, Z. L. Yang, and Q. C. Zeng, 1998: The Project for Intercomparison of Land-surface Parameterization Schemes (PILPS) phase 2(c) Red-Arkansas River basin experiment: 2. Spatial and temporal analysis of energy fluxes. *Global and Planetary Change*, **19,** 137-159.

Liou, Y. A., J. F. Galantowicz, and A. W. England, 1999: A land surface process radiobrightness model with coupled heat and moisture transport for prairie grassland. *Ieee Transactions on Geoscience and Remote Sensing*, **37,** 1848-1859.

Loveland, T. R., B. C. Reed, J. F. Brown, D. O. Ohlen, Z. Zhu, L. Yang, and J. W. Merchant, 2000: Development of a global land cover characteristics database and IGBP DISCover from 1 km AVHRR data. *International Journal of Remote Sensing*, **21,** 1303-1330.

Mitsch, W. J. and J. G. Gosselink, 2000: *Wetlands*. New York City, NY, John Wiley.

Mohr, K. I., J. S. Famiglietti, A. Boone, and P. J. Starks, 2000: Modeling soil moisture and surface flux variability with an untuned land surface scheme: A case study from the Southern Great Plains 1997 Hydrology Experiment. *Journal of Hydrometeorology*, **1,** 154-169.

Nijssen, B., I. Haddeland, and D. P. Lettenmaier, 1997: Point evaluation of a surface hydrology model for BOREAS. *Journal of Geophysical Research-Atmospheres*, **102,** 29367-29378.

Philip, J. R. and D. De Vries, 1957: Moisture movement in porous materials under temperature gradients. *Transactions, American Geophysical Union*, **38,** 222-232.

Philip, J. R., 1957: Theory of infiltration, 1. The infiltration equation and its solution. *Soil Science*, **83,** 345-357.

——, 1987a: Inverse solution for one-dimensional infiltration and ratio A/K1. *Water Resources Research*, **26,** 2023-1017.

——, 1987b: The Infiltration Joining Problem. *Water Resources Research*, **23,** 2239-2245.

Pitman, A. J. and A. Henderson-Sellers, 1998: Recent progress and results from the project for the intercomparison of landsurface parameterization schemes. *Journal of Hydrology*, **213,** 128-135.

Pitman, A. J., A. Henderson-Sellers, C. E. Desborough, Z. L. Yang, F. Abramopoulos, A. Boone, R. E. Dickinson, N. Gedney, R. Koster, E. Kowalczyk, D. Lettenmaier, X. Liang, J. F. Mahfouf, J. Noilhan, J. Polcher, W. Qu, A. Robock, C. Rosenzweig, C. A. Schlosser, A. B. Shmakin, J. Smith, M. Suarez, D. Verseghy, P. Wetzel, E. Wood, and Y. Xue, 1999: Key results and implications from phase 1(c) of the Project for Intercomparison of Land-Surface Parametrization Schemes. *Climate Dynamics*, **15,** 673-684.

Rossi, C. and J. R. Nimmo, 1994: Modeling of Soil-Water Retention from Saturation to Oven Dryness. *Water Resources Research*, **30,** 701-708.

Schaake, J., Q. Duan, V. Koren, and A. Hall, 2001: Toward improved parameter estimation of land surface hydrology models through the Model Parameter Estimation Experiment (MOPEX). *Soil-Vegetation-Atmosphere Transfer Schemes and Large-Scale Hydrological Models*, Maastricht, The Netherlands, IAHS Pblishing, 91-97.

Schotanus, P., F. T. M. Nieuwstadt, and H. A. R. Debruin, 1983: Temperature-Measurement with a Sonic Anemometer and Its Application to Heat and Moisture Fluxes. *Boundary-Layer Meteorology*, **26,** 81-93.

Shao, Y. P. and A. Henderson-Sellers, 1996: Validation of soil moisture simulation in landsurface parameterisation schemes with HAPEX data. *Global and Planetary Change*, **13,** 11-46.

Slater, A. G., C. A. Schlosser, C. E. Desborough, A. J. Pitman, A. Henderson-Sellers, A. Robock, K. Y. Vinnikov, K. Mitchell, A. Boone, H. Braden, F. Chen, P. M. Cox, P. de Rosnay, R. E. Dickinson, Y. J. Dai, Q. Duan, J. Entin, P. Etchevers, N. Gedney, Y. M. Gusev, F. Habets, J. Kim, V. Koren, E. A. Kowalczyk, O. N. Nasonova, J. Noilhan, S. Schaake, A. B. Shmakin, T. G. Smirnova, D. Verseghy, P. Wetzel, X. Yue, Z. L. Yang, and Q. Zeng, 2001: The representation of snow in land surface schemes: Results from PILPS 2(d). *Journal of Hydrometeorology*, **2,** 7-25.

Stieglitz, M., D. Rind, J. Famiglietti, and C. Rosenzweig, 1997: An efficient approach to modeling the topographic control of surface hydrology for regional and global climate modeling. *Journal of Climate*, **10,** 118-137.

Tanner, B. D. and J. P. Greene, 1989: Measurements of sensible heat flux and water vapor fluxes using eddy correlation methods. DAAD 09-87, 94 pp.

Twine, T. E., W. P. Kustas, J. M. Norman, D. R. Cook, P. R. Houser, T. P. Meyers, J. H. Prueger, P. J. Starks, and M. L. Wesely, 2000: Correcting eddy-covariance flux underestimates over a grassland. *Agricultural and Forest Meteorology*, **103,** 279-300.

University of Florida-Institute of Food Agricultural Sciences. 1985. Characterization data for selected soils. Soil Science research report No. 85-1

van der Keur, P., S. Hansen, K. Schelde, and A. Thomsen, 2001: Modification of DAISY SVAT model for potential use of remotely sensed data. *Agricultural and Forest Meteorology*, **106,** 215-231.

Verseghy, D. L., N. A. McFarlane, and M. Lazare, 1993: Class - a Canadian Land-Surface Scheme for Gcms .2. Vegetation Model and Coupled Runs. *International Journal of Climatology*, **13,** 347-370.

Webb, E. K., G. I. Pearman, and R. Leuning, 1980: Correction of Flux Measurements for Density Effects Due to Heat and Water-Vapor Transfer. *Quarterly Journal of the Royal Meteorological Society*, **106,** 85-100.

Wood, E. F., D. P. Lettenmaier, X. Liang, D. Lohmann, A. Boone, S. Chang, F. Chen, Y. J. Dai, R. E. Dickinson, Q. Y. Duan, M. Ek, Y. M. Gusev, F. Habets, P. Irannejad, R. Koster, K. E. Mitchel, O. N. Nasonova, J. Noilhan, J. Schaake, A. Schlosser, Y. P. Shao, A. B. Shmakin, D. Verseghy, K. Warrach, P. Wetzel, Y. K. Xue, Z. L. Yang, and Q. C. Zeng, 1998: The Project for Intercomparison of Land-surface Parameterization Schemes (PILPS) phase 2(c) Red-Arkansas River basin experiment: 1. Experiment description and summary intercomparisons. *Global and Planetary Change*, **19,** 115-135.

Zeng, X. B., M. Shaikh, Y. J. Dai, R. E. Dickinson, and R. Myneni, 2002: Coupling of the common land model to the NCAR community climate model. *Journal of Climate*, **15,** 1832-1854.

BIOGRAPHICAL SKETCH

Brent Whitfield was born in 1978 in West Palm Beach, Florida. He received an International Baccalaureate diploma from Suncoast Community High School in 1996, after which he began his undergraduate studies at the University of Florida. In 2001, Brent graduated with a Bachelor of Science in civil engineering. In the summer of 2001 he joined the Summer Institute for Atmospheric and Hydrospheric Sciences at NASA's Goddard Space Flight Center in Greenbelt, Maryland. In the fall of 2001, Brent began his studies as a candidate for a Master of Engineering in the Department of Civil and Coastal Engineering under the tutelage of his major professor, Dr. Jennifer Jacobs.